Epitope characterization and crystal structure of GA101 provide insights into the molecular basis for type I/II distinction of CD20 antibodies

*Gerhard Niederfellner,[1] *Alfred Lammens,[2] Olaf Mundigl,[1] Guy J. Georges,[1] Wolfgang Schaefer,[1] Manfred Schwaiger,[1] Andreas Franke,[1] Kornelius Wiechmann,[1,3] Stefan Jenewein,[1] Jerry W. Slootstra,[4] Peter Timmerman,[4] Annika Brännström,[5] Frida Lindstrom,[5] Ekkehard Mössner,[6] Pablo Umana,[6] Karl-Peter Hopfner,[2] and Christian Klein[6]

[1]Pharma Research and Early Development, Roche Diagnostics GmbH, Penzberg, Germany; [2]Department of Chemistry and Biochemistry, Gene Center, Ludwig-Maximilians Universität, Munich, Germany; [3]Institut für Chemie und Biochemie, Freie Universität, Berlin, Germany; [4]Pepscan Therapeutics BV, Lelystad, The Netherlands; [5]Sidec AB, Kista, Sweden; and [6]Pharma Research and Early Development, Roche Glycart AG, Schlieren, Switzerland

CD20 is a cell-surface marker of normal and malignant B cells. Rituximab, a monoclonal antibody targeting CD20, has improved the treatment of malignant lymphomas. Therapeutic CD20 antibodies are classified as either type I or II based on different mechanisms of killing malignant B cells. To reveal the molecular basis of this distinction, we fine-mapped the epitopes recognized by both types. We also determined the first X-ray structure of a type II antibody by crystallizing the obinutuzumab (GA101) Fab fragment alone and in complex with a CD20 cyclopeptide. Despite recognizing an overlapping epitope, GA101 binds CD20 in a completely different orientation than type I antibodies. Moreover, the elbow angle of GA101 is almost 30° wider than in type I antibodies, potentially resulting in different spatial arrangements of 2 CD20 molecules bound to a single GA101 or rituximab molecule. Using protein tomography, different CD20 complexes were found to be associated with the 2 antibodies, and confocal microscopy showed different membrane compartmentalization of these subpopulations of the cellular CD20 pool. Our findings offer a possible molecular explanation for the different cellular responses elicited by type I and II antibodies. (*Blood*. 2011;118(2):358-367)

Introduction

The B cell–specific, 35-kDa integral membrane protein CD20 is clinically validated as an immunotherapy target for B-cell lymphomas and autoimmune diseases. CD20 consists of large, intracellular, amino- and carboxyterminal portions connected by 4 membrane-spanning domains. The only extracellular portions are 2 short loops from positions 72-80 and from 142-182. Its high expression on malignant B cells and its reported lack of shedding from the surface[1] make CD20 an ideal target for antibody-mediated killing. Anti-CD20 antibodies are believed to mediate the therapeutic effect by activation of complement-dependent cytotoxicity (CDC) and largely by antibody-dependent cellular cytotoxicity exerted by recruitment of innate immune effector cells expressing the Fcγ receptor IIIa.[2] Obinutuzumab (GA101) is a glyco-engineered, humanized monoclonal anti-CD20 antibody used in clinical trials. Reduced fucosylation of its Fc portion optimizes binding of GA101 to low- and high-affinity variants of the Fcγ receptor IIIa, and therefore improves the potency of antibody-dependent cytotoxicity.[3]

Rituximab is a monoclonal anti-CD20 antibody that pioneered targeted cancer therapy. It redistributes CD20 molecules into lipid rafts, which is thought to be the molecular basis for its efficient engagement of complement factors.[4] This property is shared by all of the so-called type I CD20 antibodies and, together with other differences in the in vitro properties, has led to the distinction between type I and type II CD20 antibodies.[5] Type II CD20 antibodies such as tositumomab or GA101 induce less lipid raft translocation of CD20, and therefore are also less-potent mediators of CDC; instead, they are more effective in triggering homotypic cell aggregation and direct cell death. The exact nature of the cellular events underlying these biologic responses is poorly understood. The results of a recent study suggested that both phenomena are inherently linked through peripheral actin relocalization on antibody binding, and that the ensuing nonapoptotic cell death is caused by swelling and disintegration of lysosomes.[6]

The molecular basis of the distinction between type I and type II antibodies has not been established. So far, crystal structures of Fab fragments in complex with a cyclic epitope peptide have only been published for type I antibodies. Complexes of rituximab[7] and C2H7,[8] another chimeric type I antibody from which ocrelizumab is derived, show that an Ala-Asp-Pro-Ser (ANPS) motif at position 170-173 within the second half of the larger extracellular loop is the core epitope. Epitope-mapping and mutagenesis experiments also confirmed the key role of Ala170 and Pro172 within the ANPS motif for other mouse-derived anti-CD20 antibodies.[9,10] Most anti-CD20 antibodies seem to target the region around position 170-173 of the larger extracellular loop, whereas the type I antibody ofatumumab binds a discontinuous epitope to which the smaller extracellular loop of CD20 (position 72-80) and a more aminoterminal region of the large loop (position 159-166) contribute.[10]

In the present study, we revealed differences in the molecular interaction of CD20 with type I and II antibodies. We fine-mapped the core epitope of various type I and II antibodies using Pepscan

Submitted September 8, 2010; accepted March 15, 2011. Prepublished online as Blood First Edition paper, March 28, 2011; DOI 10.1182/blood-2010-09-305847.

An Inside *Blood* analysis of this article appears at the front of this issue.

*G.N. and A.L. contributed equally to this study.

The online version of this article contains a data supplement.

The publication costs of this article were defrayed in part by page charge payment. Therefore, and solely to indicate this fact, this article is hereby marked "advertisement" in accordance with 18 USC section 1734.

methodology, and confirmed the results by site-directed mutagenesis. The first X-ray structure for a type II CD20 antibody with a cyclic epitope peptide revealed a substantially different binding mode of GA101. Finally, we visualized CD20 complexes formed on intact cells in the presence of type I or II antibodies using protein tomography and investigated their membrane compartmentalization by confocal microscopy of living cells. Our results suggest that type I and II antibodies form different molecular assemblies with separate subpopulations of CD20 molecules on lymphoma cells, which could explain their functional differences.

Methods

Cells and antibodies

All cell lines were obtained from the German Collection of Microorganisms and Cell Cultures (DSMZ) or ATCC and cultured as recommended. H299/B1 and LT20 were purchased from Becton Dickinson and Axxora, respectively. Other antibodies were provided by Roche Glycart and Biologics Research Penzberg.

Peptide-based ELISA

The mini-Pepscan method was performed as described previously[11] (see supplemental Methods, available on the *Blood* Web site; see the Supplemental Materials link at the top of the online article). Peptides (4291) representing both extracellular CD20 loops were synthesized. For all 8-mers covering the large extracellular loop (aa 142-187), the ratio between their average binding value and that of all peptides was determined. The binding epitope is identified as a sliding window of adjacent 8-mer sequences with a ratio > 1. For fine analysis of each residue in the core epitope, the binding values of peptides in which a particular position was replaced by all other possible 18 amino acids were divided by the binding value for the native sequence.

Site-directed mutagenesis

The CD20 cDNA was cloned in-frame with a carboxyterminal hemagglutinin tag into KspI/NotI sites of pMH (Roche Applied Science). See supplemental Methods for primers used for site-directed mutagenesis with the QuikChange kit (Stratagene).

FACS analysis

Freestyle 293-F cells (Invitrogen) were cotransfected at a 2:1 ratio with pLNGFR (Miltenyi Biotec) encoding a cell-surface marker and wild-type or mutated CD20 cDNAs. On day 2 after transfection, cells were costained with a PE-labeled mouse anti-LNGFR antibody and anti-CD20 antibodies. LT20 and H299/B1 were directly FITC labeled, and the others were detected by a FITC-conjugated goat anti–human IgG (Jackson ImmunoResearch Laboratories). The analysis was focused on successfully transfected, intact cells by gating on viable cells with $> 10^4$ PE signal intensity. The average PE signal for each transfection was used to assess relative transfection efficiency. The half-maximal effective concentration (EC_{50}) values were calculated from the saturation binding curves of 3 independent experiments.

Crystallization

The crystallization procedure is described in detail in supplemental Methods. In brief, the GA101 Fab structure was solved by molecular replacement to a limiting resolution of 2.5 Å. The obtained structure was subsequently used to solve at a 1.6 Å resolution the structure of the Fab fragment in complex with an epitope peptide mimicking the large extracellular loop of CD20.

Protein tomography

Antibody-treated or -untreated Ramos RA1 cells were fixed with 4% paraformaldehyde by adding an equal volume of double-strength fixative to the culture medium. After embedding and cryosectioning of cells, anti-CD20 antibodies were immunolabeled with rabbit anti–human IgG and protein A-gold. Protein tomography analyses were done by Sidec Technologies AB (see supplemental Methods).

Live cell labeling and confocal microscopy

Z138 cells were seeded at 1.5×10^6/mL in medium on poly-L-ornithine–coated glass coverslips and stained with 5μg/mL of dye-labeled antibody at either 4°C or 37°C. Cells were washed twice and in some cases were fixed with 4% paraformaldehyde for 20 minutes. Images were taken on a TCS SP2/MP confocal laser scanning microscope (Leica) at 100× magnification and 1.46 numerical aperture. Selective spectral detector emission band passes for each dye were used in sequential scanning mode. The detection pinhole size was set to 1 Airy unit and the voxel size was between 28 and 33 nm.

Results

Type I and II antibodies recognize overlapping CD20 epitopes differently

To better understand the molecular differences in the way type I and II antibodies interact with similar epitopes, we fine-mapped their epitopes using Pepscan technology. Whereas for type I antibodies, the epitope "footprint" started around Ile162 and generally did not reach beyond Asn176, a right shift was seen with type II antibodies (Figure 1A). For GA101, the footprint started around position Ala167 and extended to Pro178. A similar right shift was seen with the parental B-Ly1 antibody and also for a completely unrelated type II antibody, H299/B1.

To determine whether the epitopes are not only slightly shifted but also differently recognized, we assessed the effect of replacing each residue between positions 142 and 187 by all other possible amino acids. We found that the core epitope of GA101 and other type II antibodies was formed by residues 172-178 of CD20, whereas the epitope region of rituximab and other type I antibodies were located more aminoterminally, comprising residues 168-175, with 170-173 contributing most essentially (Figure 1B). A contribution of more carboxyterminal residues to the core epitope of type II antibodies was indicated by the fact that GA101, H299/B1, BHH2A, and B-Ly1 did not tolerate most exchanges of Asn176, Ser177, and P178, whereas the type I antibodies rituximab, LT20, and 2H7 were insensitive to substitutions at these positions (Figure 1B).

Regarding the role of Asn171, the Pepscan analyses also revealed a major difference between rituximab and GA101. For rituximab, any replacement of this residue, except for histidine, resulted in substantial loss of binding affinity, whereas for GA101 (and the related antibodies BHH2A and B-Ly1), substitutions were well tolerated or often even improved binding. Another type II antibody, H299/B1, tolerated 4 of 18 substitutions well. In summary, despite targeting the same region on CD20, type I and II antibodies appear to recognize this epitope in a different way.

Epitope analysis by site-directed mutagenesis of native CD20

To confirm these data, we introduced selected amino acid exchanges in the context of the native CD20 protein and tested by FACS their effect on binding of the different antibodies. Based on the Pepscan results, exchanges of Asn171 were chosen because they were expected to differentially affect binding of rituximab and

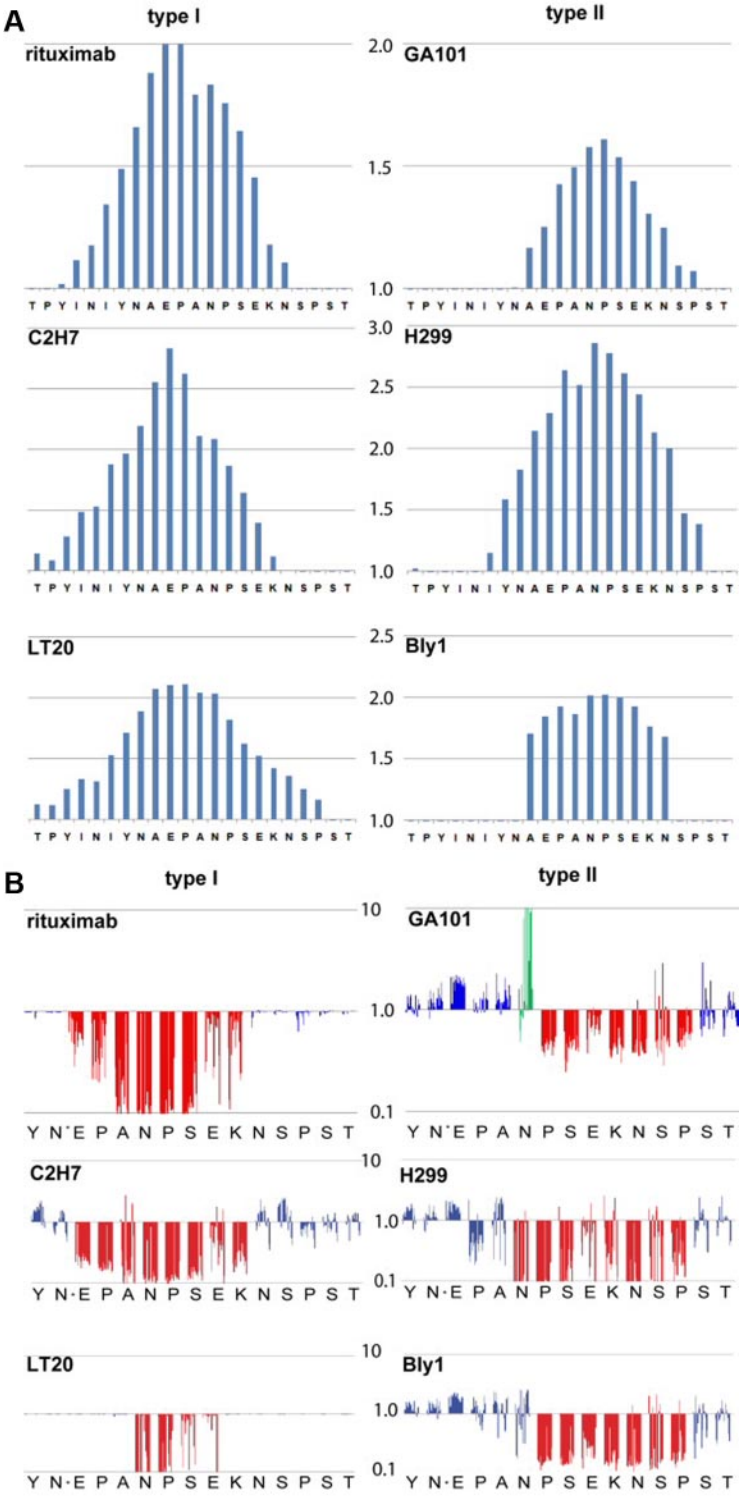

Figure 1. Pepscan analysis of the epitopes of rituximab and GA101. (A) Epitope footprints of type I (rituximab, 2H7, and LT20) and type II (GA101, H299/B1, and B-Ly1) antibodies: 39 different overlapping 8-mer sequences covering position 142-187 in CD20 were synthesized. The ratio between the average binding value in all peptides containing a particular 8-mer sequence and the average binding value of all 4291 peptides was calculated. When the ratio was > 1, all peptides containing that particular 8-mer sequence had a binding value above average. Consecutive 8-mer sequences with a ratio > 1 indicate the presence of the epitope. (B) Fine mapping of the binding contribution of each residue within epitopes of the same type I and II antibodies as in panel A. A peptide library was synthesized in which, with the exception of C167 and C183, the residues in every position between Y165 and S185 were replaced by all possible alternative natural amino acids except for cysteine. Therefore, 18 single substituted peptides per position were synthesized and their binding value relative to the native CD20 loop peptide (position 142-187 in CLIPS) was determined. Substitutions negatively affecting binding result in a ratio < 1, and the respective bars in the graph are colored red. If replacements clearly improved binding, the ratios were > 1 and the corresponding bars are colored green.

GA101. Upon transient transfection of wild-type and mutant CD20 cDNAs, similar amounts of mRNA were detected by quantitative RT-PCR (supplemental Figure 1A). With few exceptions, the amounts of protein detected by Western blot analysis were comparable to wild-type CD20 (supplemental Figure 1B). For unknown reasons, the S177A mutant protein was always expressed at higher levels than wild-type CD20. The C167S exchange, which abrogates the internal disulfide bridge (C167-C183) of the large extracellular loop, seems to completely destabilize CD20, because this variant was barely detectable by Western blot analysis.

The representative FACS-binding curves in Figure 2 show that amino acid exchanges affect the type I antibodies differently than the type II antibodies. Whereas rituximab and LT20 did not bind any of the 8 variants with Asn171 exchanges, GA101 and H299/B1 tolerated several substitutions at that position fairly well. GA101 binding was unaffected by introducing alanine or isoleucine, and seemed rather improved by serine, threonine, or valine as substituents. These results confirm that for the type II antibodies, Asn 171 is not at the center of the epitope. Moreover, in agreement with the observation of a carboxyterminal shift of the core epitope, we

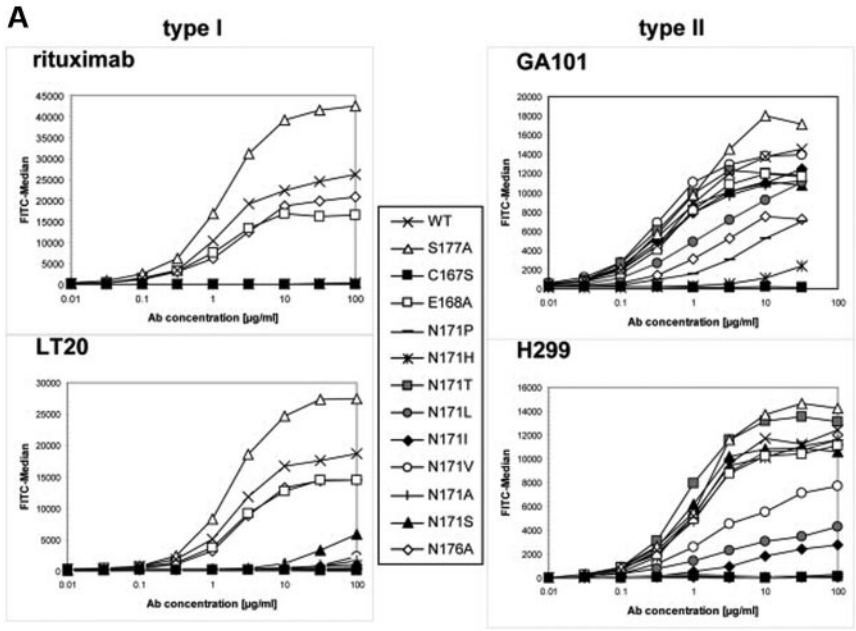

Figure 2. Binding of rituximab and GA101 to mutant CD20 variants on intact cells. (A) FACS-binding curves of rituximab and GA101. Point-mutated CD20 variants were transiently transfected in Freestyle 293-F cells. By gating on live cells with high transfection efficiency, FACS-binding curves were determined for the indicated antibodies. It was readily apparent that binding of the type I antibodies rituximab and LT20 was completely abolished by each of the 8 different substitutions of the N171 residue, whereas exchanges at the more peripheral positions E168, N176, and S177 were well tolerated. In contrast to this, binding of the type II antibodies GA101 and H299/B1 was less affected by many substitutions of N171, but was weakened by the N176A exchange. (B) Table of normalized EC_{50} values for rituximab, LT20, GA101, and H299/B1. The average EC_{50} values from 3 independent experiments were calculated for different CD20 variants using 2 type I (rituximab and LT20) and 2 type II antibodies (GA101 and H299/B1). To average data from separate experiments, all values were normalized by calculating the ratios of EC_{50} mutant:EC_{50} wt. The standard deviations for the ratios calculated from the 3 separate experiments are indicated.

B

EC50 values normalized to wt				
	Rx*	LT20*	GA101*	H299*
E168A	0.8 ± 0.1	1.0 ± 0.1	0.8 ± 0.2	0.7 ± 0.3
N171S	wb	wb	0.7 ± 0.3	0.6 ± 0.2
N171A	wb	wb	1.1 ± 0.3	1.3 ± 0.5
N171V	wb	wb	0.7 ± 0.3	wb
N171I	wb	wb	0.9 ± 0.1	wb
N171L	wb	wb	3.1 ± 1.1	wb
N171T	wb	wb	0.6 ± 0.1	0.5 ± 0.2
N171H	wb	wb	wb	1.0 ± 0.5
N171P	wb	wb	11.4	wb
N176A	1.3 ± 0.2	1.3 ± 0.1	3.1 ± 0.8	wb
S177A	1.2 ± 0.3	1.4 ± 0.7	1.3 ± 0.6	1.7 ± 1.2
wt	1.0	1.0	1.0	1.0

* = average of 3 independent repeats ± standard deviation
wb = weak binding; due to low affinity of antibody to CD20 variant a binding plateau was not reached at concentrations up to 100µg/ml and curve fitting was not possible.

found that binding of both type II antibodies was negatively affected by the N176A exchange, whereas all type I antibodies tolerated this exchange well (Figure 2). Overall, the FACS data corroborated the general findings from our Pepscan analysis, also indicating that the topology of the large extracellular loop of CD20 lends itself to mimicry by chemical linkage of peptides onto scaffolds (CLIPS) technology.

Binding of GA101 and rituximab to a cyclic epitope peptide

To initiate structural studies of epitope recognition by GA101, we next investigated its binding to a cyclic epitope peptide previously used for cocrystallization with rituximab.[7] Determination of its stoichiometric binding ratio with isothermal calorimetry showed that this peptide was also fully active in binding to GA101. Furthermore, the thermodynamic values indicated high enthalpic contribution to the interaction. In agreement with this, the dissociation constant (K_D) value of GA101 increased in a temperature-dependent fashion (2µM at 15°C, 7µM at 25°C, and 28µM at 37°C). Because rituximab has a lower affinity for this peptide, we could determine a K_D value for rituximab only at 15°C (27.7µM). A higher apparent affinity of GA101 versus rituximab for this peptide was confirmed by surface plasmon resonance measurements (data not shown). However, on intact non-Hodgkin lymphoma cells, the binding affinities of both antibodies for native CD20 molecules were comparable and several orders of magnitude higher (~ 5nM) than that for the isolated epitope peptide.[3] This may have been due to avidity effects and the proper pre-orientation of the epitope in the native protein context.

Structures of GA101 Fab and its complex with the CD20 epitope peptide

To reveal differences in epitope recognition between type I and II antibodies, we determined crystal structures of the GA101 Fab alone and in complex with the cyclic epitope peptide (Table 1 and Figure 3A). In the structure of the Fab:peptide complex, we could build all residues of the peptide into well-defined density except the 2 most aminoterminal residues (Asn163 and Ile164; Figure 3B). Interestingly, we found an additional strong electron density at the interface of the GA101 Fab and the CD20 peptide, which we interpreted as a chloride ion. This was coordinated by hydrogen bonds to residues of the heavy- and light-chain complementarity–determining regions of GA101, Tyr101 (L3), Asn35 (H1), and Arg50 (H2), but not to atoms of the CD20 peptide (Figure 3C).

Table 1. Summary of crystallographic data and refinement statistics.

	GA101 Fab	GA101 Fab: CD20 peptide
Data collection and analysis		
Beamline	ID23-2 (ESRF)	ID23-1 (ESRF)
Wavelength	0.9724 Å	1.0000 Å
Space group	C2	C2
Cell	a = 273.14 Å	a = 84.05 Å
	b = 38.04 Å	b = 85.90 Å
	c = 90.22 Å	c = 72.87 Å
	$\alpha = \gamma = 90°$	$\alpha = \gamma = 90°$
	$\beta = 98.89$	$\beta = 116.34$
Resolution (last shell), Å	35-2.5 (2.66-2.5)	50.0-1.6 (1.7-1.6)
Observed reflections (last shell)	100523 (30 376)	218321 (59 284)
Completeness (last shell)	94.2% (84.3%)	96.7% (91.3%)
R_{sym} (last shell)	6.6 (25.3)	4.3 (19.8)
Refinement		
Resolution (Å)	35-2.5	43-1.6
Reflections (test set)	31 465 (2000)	60 342 (2000)
No. of atoms		
Fab	6672	3542
Peptide		196
Ion		1xCl^-
Water	525	761
R_{work}/R_{free}	20.41/26.85	13.73/18.74
rmsd bond/angles	0.003/0.712	0.004/0.946
Ramachandran		
Most favored	87.7%	89.9%
Allowed	11.9%	9.7%
Generously allowed	0.1%	0.3%
Disallowed	0.3%	0.3%
PDB accession numbers	3PP3	3PP4

PDB indicates Protein Data Bank.

Interaction between GA101 Fab and CD20 epitope peptide

Epitope mapping had shown that, compared with type I antibodies, GA101 displays binding specificity for an extended sequence ^{170}ANPSEKNSP^{178}. Although residue Asn171 lies within this epitope footprint and in the crystal structure forms hydrogen bonds to the backbone carbonyl of Asn96 (L3) of GA101 and Ser173 of the peptide (Figure 3C), it was clearly not essential for binding of GA101 to CD20. Consistent with the overall hydrophobic environment at this position (Figure 3C), replacing Asn171 with a small aliphatic amino acid such as valine, isoleucine, or leucine increased GA101 binding in Pepscan (Figure 1B). Similarly mutating Asn171 to serine or threonine enhanced GA101 binding, probably by improving the steric arrangement for possible hydrogen bonding. The crystal structure suggests binding contributions by the more carboxyterminal residues ^{174}EKN^{176} of the extended epitope footprint for GA101 binding, because they were embedded in a dense hydrogen bond network (Figure 3C).

Structural comparison of the epitope peptide complexes of GA101, rituximab, and C2H7

The remarkably extended core epitope of GA101 (^{170}ANPSEKNSP^{178}) increased the buried surface area between GA101 and the CD20 peptide to 445.4 Å^2, compared with 411.4 Å^2 and 403.4 Å^2 for rituximab and C2H7, respectively. In addition, the altered epitope recognition of GA101 resulted in a completely different binding topology compared with type I antibodies. Superposition of the Fab structures of GA101 with the known structures of rituximab and C2H7 using the bound epitope peptide as a reference showed that rituximab and C2H7 bound the peptide in a comparable orientation (Figure 4A). The type II antibody GA101, however, bound the peptide in a relative orientation that was rotated 90° clockwise around its middle axis defined by the pseudo dyads, and was also tilted approximately 70° toward the carboxyl terminus of the peptide. These completely different binding orientations offer an explanation at the molecular level for the remarkable lack of positive contribution of Asn171 to CD20 binding by GA101 observed in our epitope studies (Figure 1B and Figure 2). Whereas the side chain of this asparagine residue reached deep into the bottom of a binding pocket formed by 4 complementarity-determining regions of rituximab, it was located more toward the surface of the interaction site in the GA101 Fab complex and contributed to binding merely with a hydrogen bond to the backbone carbonyl of Asn96 (L3; Figure 4B). In fact, the side chain of Asn171 would clash with various residues of GA101 if it did not fold back on the peptide itself by hydrogen bonding with the hydroxyl group of Ser173 (Figure 3C). This intramolecular hydrogen bond puts steric constraints on the peptide conformation and may explain why in the Pepscan setting, many substitutions of Asn171 showed improved binding.

In addition to the shifted binding orientation, GA101 possesses a different elbow angle compared with rituximab and C2H7. The elbow angle relates VH to VL and CH to CL via the 2 pseudo-dyad axes, and thereby affects the spatial arrangement of 2 bivalently bound epitope molecules. With 167°, the elbow angle of GA101 is ~ 30° wider than those of rituximab (139°) and C2H7 (141°; Figure 4C). The fact that mutating residue valine 11 of the elbow hinge region of GA101 to a more bulky leucine residue reduced the ability of GA101 to induce direct cell death, one of the hallmarks of a type II antibody,[3] suggests a functional role for this wider elbow angle. Replacing valine with the larger leucine likely pushed away the opposing F125, thereby narrowing the elbow angle, as we observed for rituximab and C2H7 (Figure 4C).

In summary, our crystal data confirmed that GA101 binds to CD20 in a different orientation compared with type I antibodies. In combination with a wider elbow angle, this could favor distinct 3D arrangements and conformations of bound CD20 molecules.

3D visualization of CD20-antibody complexes in situ by protein tomography

To visualize different CD20 complexes bound to rituximab and GA101, we used protein tomography, a technique that allows 3D imaging of protein conformations in situ.[12] In agreement with a higher number of cellular-binding sites for type I versus type II antibodies, 3-fold more immunogold markers were detected on slides from samples treated with rituximab versus GA101. Immunogold markers were found to be associated with repeating volume entities of similar bipartite shapes (supplemental Figure 2E). The larger part of these entities, to which the antibodies bound, was interpreted as the extracellular and transmembrane portion of a CD20 molecule, whereas the smaller part could represent the less structured and therefore less electron-dense intracellular portion (supplemental Figure 2F). Reconstructed, immunogold-labeled protein complexes were sorted into 4 categories based on their size and structure (Table 2). Both antibodies were found engaged with tetrameric structures, but only rituximab was equally often bound to large, network-like structures of unidentified proteins (supplemental Figure 2G-H). Of the tetrameric complexes, 2 different organization types classified as open and closed conformations were discernible (Figure 5). Whereas rituximab was only found associated with the open conformation, both conformations were observed with GA101. Monovalent binding, and less frequently also

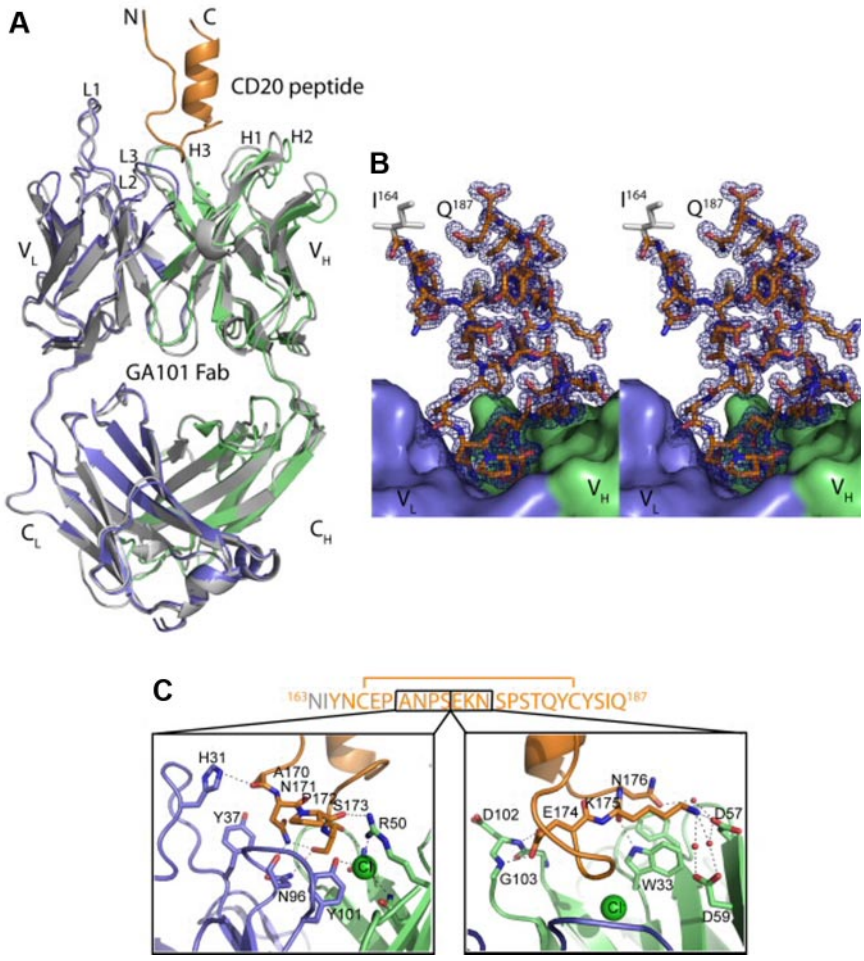

Figure 3. Crystal structure of the GA101-CD20 epitope peptide complex. (A) Overall structure of the complex as a ribbon model. The GA101 Fab is shown with the light chain in blue, the heavy chain in green, and the CD20 epitope peptide in orange. The superimposed GA101 Fab alone showed only minor structural changes and is colored in gray. (B) Stereo view of the final 2FO-FC electron density map for the bound CD20 epitope peptide countered at 1σ. The ordered part of the peptide comprising residues 163-187 is shown as color-coded stick model and the Fab fragment as surface representation. (C) Detailed view of the CDR of GA101 binding to the CD20 epitope peptide (sequence) showing the hydrogen bonds mediating the interaction. The left panel shows the interactions of residues ^{170}ANPS^{173} and the right panel hydrogen network of residues ^{174}EKN^{176}. A bound chloride ion at the interface is depicted as a green sphere. Color coding of GA101 and CD20 is the same as in panel A.

bivalent binding, was observed with both antibodies. In summary, the protein tomography experiments imply that complexes formed by rituximab and GA101 with CD20 on intact cells do indeed differ with respect to their multimeric state and conformations.

Confocal microscopy of CD20-antibody complexes

We next investigated by confocal microscopy whether the distinct differences in molecular recognition of CD20 by GA101 versus rituximab result in recognition or stabilization of different subpopulations of CD20 complexes on intact cells. When GA101 and rituximab labeled with different fluorescent dyes were added simultaneously at 4°C to Z138 cells, both antibodies largely colocalized at homotypic adhesion sites (data not shown). However, within 30 minutes of incubation at 37°C, most of the rituximab immunoreactivity redistributed from the homotypic adhesion sites to adjacent, more lateral regions. After 1 hour, the 2 staining patterns showed little overlap in isolated Z138 cells (Figure 6AI-III) and in aggregated Z138 cells (Figure 6CI-III). As expected, in control experiments for which the same antibody labeled with 2 different fluorophores was used, the staining patterns completely overlapped (Figure 6AIV-VI and VII-IX, respectively). Therefore, GA101 and rituximab induce redistribution of CD20 complexes into separate membrane compartments. Whereas GA101-associated CD20 complexes massively accumulated at sites of cell-cell contact (Figure 6AII,CII), those bound to rituximab concentrated in big spots, likely representing large assemblies of coalesced lipid rafts (Figure 6AI,CI). A time-lapse video (see supplemental Video) demonstrates different dynamic behavior of the 2 subpopulations. Whereas large membrane spots marked by rituximab showed a highly dynamic behavior, also transiently trafficking in and out of cell-cell contact sites, GA101-associated CD20 complexes appeared completely static as if trapped in membrane areas of cell-cell contact. A similar separation of GA101- versus rituximab-associated CD20 complexes was also observed in Ramos cells (Figure 6BI-III), a Burkitt lymphoma cell line, and to a lesser extent in normal B cells (Figure 6BIV-VI).

Discussion

The molecular basis for the fundamentally different cellular effects of type I and II anti-CD20 antibodies despite their largely overlapping binding regions has remained unclear. Our epitope fine-mapping studies yielded 2 intriguing results: (1) the Asn171 of CD20 plays little role in GA101 binding, whereas (2) more carboxyterminally located residues such as Asn176 contribute to its binding (Figure 4B). Both findings held true for other type I (LT20 and 2H7) and type II antibodies (H299/B1), suggesting that these are properties that determine type I and II characteristics. Our crystal structure of a type II antibody/epitope peptide complex offers a molecular explanation for these findings by showing that the shift of the core epitope results from a fundamentally different

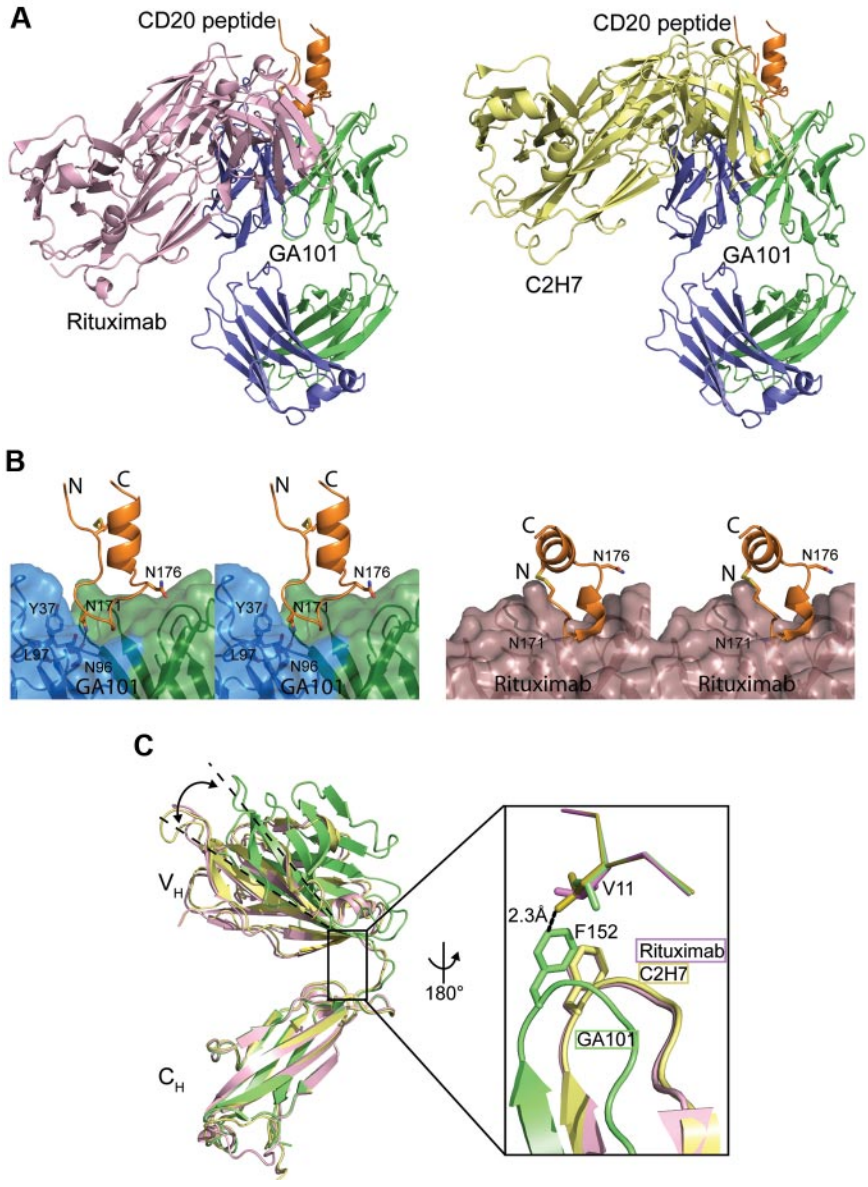

Figure 4. Comparison of the GA101-CD20 epitope-binding topology with other CD20 antibodies. (A) Superposition of CD20 epitope peptide bound rituximab (left) and C2H7 (right) onto the GA101 complex with respect to the peptide. In relation to both type I antibodies, GA101 was rotated 90° around the Fab middle axis and tilted ~ 70° toward the carboxyl terminus of the epitope peptide. The GA101 Fab is shown with the light chain in blue, the heavy chain in green, and the CD20 epitope peptide in orange. The Fab fragment of rituximab is colored pink and that of C2H7 in yellow. (B) Stereo view of the position of the peptide residue N^{171} within the antigen-antibody interaction surface of GA101 (left) versus rituximab (right). In the epitope peptide complex with rituximab, the side chain of Asn176 made no contact with the antibody and therefore did not contribute to binding. In the crystal structure with GA101, the side chain of Asn176 extended toward a pocket formed by several residues (W33, F51, D57, and D59) of the heavy chain of GA101. Exchanging Asn176 to alanine substantially reduced the binding signal in Pepscan experiments and caused a small but reproducible impairment of GA101 binding on intact cells. (C) Superposition of the V_H domains of GA101, rituximab, and C2H7 with respect to the constant region. Whereas rituximab and C2H7 had a similar elbow angle of ~ 140°, GA101 had an elbow angle of 167°. Color coding is the same as in panel A.

Table 2. CD20 antibody complexes visualized by electron tomography.

Sample	GA101	Rituximab
Tilt series		
Total recorded	25	15
Processed	24	14
Immunogold markers		
Total found	98	194
CD20 complexes	23	49
Multimeric states of analyzed CD20 complexes		
Tetramers	14	16
Higher-order multimers	4	1
Networks	0	12
Unassigned	5	20
Subanalysis: valency of Ab binding		
Monovalent Ab binding	12	5
Bivalent Ab binding	1	5
Subanalysis: tetramer conformations		
Multimers	2	1
Tetramers	11	13
Open conformation	7	10
Closed conformation	4	0
Conformation not defined	0	3

orientation of GA101 with respect to CD20. In contrast to the rituximab/epitope complex, Asn171 of CD20 is not at the center of the GA101-peptide interface, but rather is located toward the periphery of the interaction surface and does not significantly contribute to binding. One implication is that mutations resulting in a substitution of Asn171 cause resistance to rituximab therapy, whereas GA101 binding likely remains unaffected. However, mutations involving the rituximab epitope have been reported to be a rare event in diffuse large B-cell lymphoma, occurring only in 1 of 264 de novo and 1 of 15 relapsed cases.[13] In the X-ray structure, the space available for the residue in position 171 is just big enough to fit the side chains of serine, threonine, and valine, which were the best tolerated substitutions in the FACS-binding experiments. In fact, binding of GA101 to wild-type CD20 forces the side chain of Asn171 to fold back on the peptide itself by hydrogen bonding with the hydroxyl group of Ser173. This might put steric constraints on the conformation of the large extracellular loop of CD20. In the Pepscan setting, more substitutions of Asn171 improved GA101 binding than in the FACS-binding assays, possibly due to the greater flexibility of the cyclic peptide

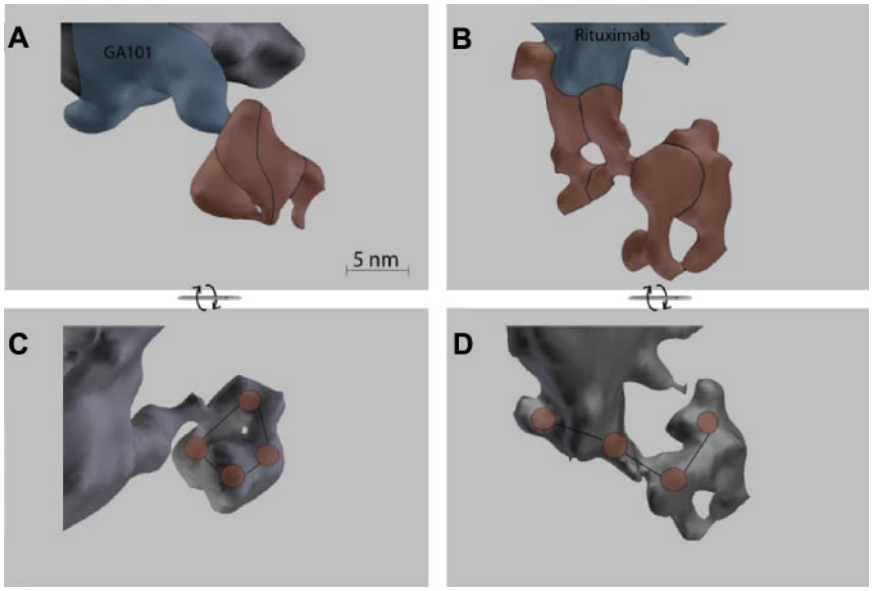

Figure 5. Tomograms of closed and open CD20 tetramers. Tomograms showing 1 example each of a closed (A and C) and open (B and D) conformation CD20 tetramer on Ramos RA1 cells. In the color-annotated tomograms (A and B), the parts of the tomogram representing the mAbs are shown in blue and the parts representing the CD20 multimers are shown in red. The approximate borders of individual CD20 entities within the tetramers are indicated by black lines. In the rotated views in panels C and D, the center of each CD20 molecule is marked with a red circle. Black lines connect the centers of the CD20 entities of a tetramer.

compared with native CD20. Furthermore, in the context of the native protein inserted in the cell membrane, steric constraints imposed by GA101 binding might only be compatible with the conformation of a certain subpopulation of CD20 molecules, such as those present in homotypic adhesion regions, but not with those found in lipid rafts.

In the course of humanization, the leucine in Kabat position 11 of the murine B-Ly1 antibody was replaced by valine. Because reintroducing leucine has been shown to weaken the type II character of GA101,[3] the 30° wider elbow angle of GA101 versus rituximab and C2H7 could be another contributing factor to the type II versus type I distinction. The smaller side chain of valine in position 11 allows the phenylalanine residue in position 152 to move out, thereby opening up the elbow angle, whereas in B-Ly1, rituximab, and C2H7, this phenylalanine is held in place by the bulky side chains of leucine or isoleucine residues at position 11 (Figure 4C). Antigen binding has not been reported to require or induce conformational adaption of the elbow angle of a Fab fragment. In agreement with this, the same elbow angle was found in GA101 Fab structures obtained with or without epitope peptide. The primary function of the elbow angle is to enhance an antibody's ability to simultaneously bind 2 ligands arranged on a pathogen surface by allowing greater flexibility of the Fab arm.[14] Therefore, the different elbow angles of rituximab and GA101 likely influence the relative spacing of bivalently bound CD20 molecules on the cell surface. One implication of these findings is a directed strategy for generating type II antibodies by first screening for antibodies that bind a cyclic epitope peptide in which Asn171 is exchanged to, for example, a serine, and then engineering a wider elbow angle. Just opening up the elbow angle in itself is clearly insufficient to endow type II properties on a type I antibody, because a rituximab variant with valine in Kabat position 11 shows no type II characteristics and ofatumumab is a type I antibody, despite being an IgG1κ isotype with a wide elbow angle.

Whereas the conformations of the epitope peptide in crystal structures of type I and II antibodies are superimposable, the conformations of naive CD20 molecules visualized by protein tomography on intact cells appear to be different in "open" and "closed" tetramers and in the large network structures associated with rituximab. The characteristic 2:1 ratio of the maximum number of cellular binding sites for type I versus II antibodies could therefore reflect either the relative abundance of different CD20 subpopulations recognized by each type or specific steric requirements for bivalent antibody binding dictated by the combined effect of different binding orientations and elbow-hinge angles. Combined with the confocal microscopy findings, it appears that GA101 induces homotypic cell aggregation and nonapoptotic direct cell death by stabilizing fairly static CD20 complexes that form preferentially at cell-cell contact sites and might be connected to the cytoskeleton. Conversely, rituximab did not induce these same phenomena, stabilizing a completely different, highly dynamic subpopulation of CD20 molecules that could be part of large protein networks formed within coalesced membrane domains. The ability of anti-CD20 antibodies to induce complement activation has been shown to be correlated with their ability to redistribute CD20 into lipid rafts,[4] whereas the peripheral relocalization of actin is claimed to be critical for homotypic adhesion and nonapoptotic cell death induced by type II antibodies.[6] Ofatumumab (2F2) is also characterized as a type I antibody based on its ability to redistribute CD20 to lipid rafts and potently induce CDC. Pepscan data suggest[10] that ofatumumab and other human-derived anti-CD20 antibodies are unique in recognizing discontinuous epitopes composed of the small extracellular loop and a portion of the large extracellular loop that lies further aminoterminal than the rituximab epitope. Although the Fab fragment of ofatumumab has been crystallized, its binding mode remains speculative, because cocrystallization efforts with peptides derived from the small and large extracellular loop have failed.[15] In contrast to rituximab and 2H7, the CDR loops of ofatumumab form a largely hydrophobic binding pocket with a positively charged Arg residue at the bottom, suggesting that the epitope core is centered around Glu150 of CD20. Therefore, an aminoterminal shift of the epitope core compared with rituximab appears compatible with the type I character of anti-CD20 antibodies.

In summary, the first crystal structure of a type II Fab:CD20 peptide complex provides a molecular explanation for different epitope footprints and the strikingly different dependence of rituximab and GA101 on Asn171 and Asn176 for binding. Furthermore, our findings suggest that engagement by the 2 types of

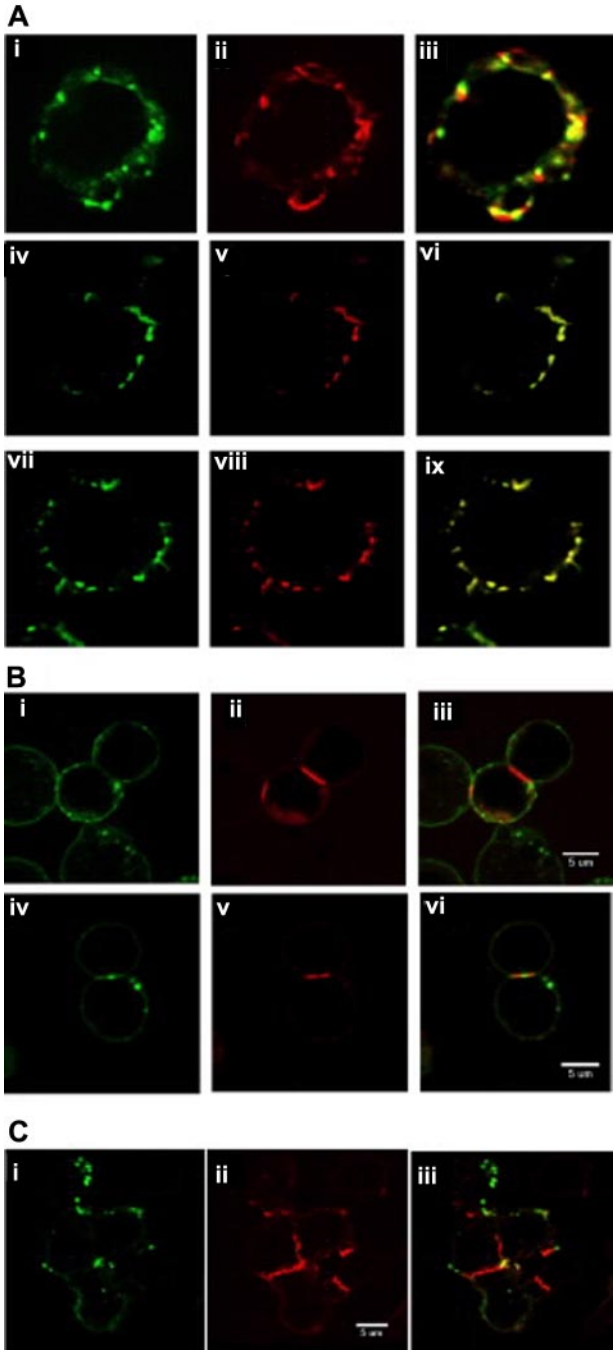

Figure 6. Confocal microscopy showing membrane compartmentalization of rituximab-associated versus GA101-associated CD20 complexes. (A) After ≥ 1 hour of incubation at 37°C with 5 μg/mL of dye-labeled antibodies, only partial colocalization of rituximab (red) and GA101 (green) was seen in isolated Z138 cells (panels i-iii), whereas control stainings with differently labeled versions of the same antibody resulted in each case in 100% colocalization (panels iv-vi for GA101 and panels vii-ix for rituximab). (B) Different membrane compartmentalization of rituximab (green) and GA101 (red) was also observed in the Burkitt lymphoma cell line Ramos (panels i-iii) and in freshly isolated normal B cells (panels iv-vi). (C) After homotypic aggregation of Z138 cells, rituximab (green) remained concentrated in large membrane spots, whereas GA101 (red) accumulated in areas of cell-cell contact, resulting in almost complete separation of the 2 labels (panels i-iii).

antibodies likely favors different conformations and spatial arrangements of bound CD20 complexes. As a consequence of this, rituximab and GA101 recognize or stabilize different subpopulations of CD20 molecules that sequester to different membrane compartments and thereby mediate different cellular responses.

Acknowledgments

We thank Hedda Herrmuth, Gabriele Klingner, and Doris Ziegler-Landesberger for excellent technical assistance with the mutagenesis analyses and the confocal microscopy experiments, respectively. We also thank Alexander Lifke for preparing primary B cells for confocal microscopy studies, the staffs of European Synchotron Radiation Facility ID23 and Swiss Light Source Paul Scherrer Institut for help with data collection, and the Max-Planck Crystallization Facility in Martinsried for crystal screening.

K.P.H. is supported by the Deutsche Forschungsgemeinschaft (Sonderforschungsbereich 646) and the German Excellence Initiative (Center for Integrated Protein Science-Munich cluster).

Authorship

Contribution: G.N. conceived and supervised the mutagenesis studies, compiled and interpreted different datasets, and wrote a large part of the paper; A.L. performed the crystallography work and also wrote and edited large sections of the paper; O.M. performed the confocal microscopy experiments; G.J.G. and W.S. contributed to analysis and interpretation of the structural data and provided guidance on the selection of the most informative amino acid exchanges in the epitope of CD20; M.S. prepared the purified GA101 Fab fragment and gave input on structural aspects; A.F. and K.W. performed the site-directed mutagenesis and FACS experiments; S.J. performed the isothermal calorimetry and surface plasmon resonance measurements with the cyclic epitope peptide; J.W.S. and P.T. designed the CLIPS library and supervised the Pepscan analysis; A.B. and F.L. performed the protein tomography study; E.M. gave intellectual input on the role of the elbow angle and provided vital reagents; and P.U., K.-P.H., and C.K. conceived the initial research plan and contributed to the interpretation of the data and to writing the paper.

Conflict-of-interest disclosure: G.N., O.M., G.J.G., W.S., M.S., A.F., and K.W. are all employees of Roche Diagnostics GmbH. C.K., P.U., and E.M. are employees of Roche Glycart AG. The remaining authors declare no competing financial interests.

Correspondence: Christian Klein, Roche Glycart AG, Wagistrasse 18, CH-8952 Schlieren, Switzerland; e-mail: christian.klein.ck1@roche.com; or Prof Karl-Peter Hopfner, Gene Center, Ludwig-Maximilians Universität, Feodor-Lynen-Str 25, 81377 Munich, Germany; e-mail: hopfner@lmb.uni-muenchen.de.

References

1. Glennie MJ, French RR, Cragg MS, Taylor RP. Mechanisms of killing by anti-CD20 monoclonal antibodies. *Mol Immunol*. 2007;44(16):3823-3837.
2. Winter MC, Hancock BW. Ten years of rituximab in NHL. *Expert Opin Drug Saf*. 2009;8(2):223-235.
3. Mössner E, Brunker P, Moser S, et al. Increasing the efficacy of CD20 antibody therapy through the engineering of a new type II anti-CD20 antibody with enhanced direct- and immune effector cell-mediated B-cell cytotoxicity. *Blood*. 2010;115(22):4393-4402.
4. Cragg MS, Morgan SM, Chan HTC, et al. Complement-mediated lysis by anti-CD20 mAb correlates with segregation into lipid rafts. *Blood*. 2003;101(3):1045-1052.

5. Beers SA, Chan CH, French RR, Cragg MS, Glennie MJ. CD20 as a target for therapeutic type I and II monoclonal antibodies. *Semin Hematol.* 2010;47(2):107-114.
6. Ivanov A, Beers SA, Walshe CA, et al. Monoclonal antibodies directed to CD20 and HLA-DR can elicit homotypic adhesion followed by lysosome-mediated cell death in human lymphoma and leukemia cells. *J Clin Invest.* 2009;119(8):2143-2159.
7. Du J, Wang H, Zhong C, et al. Structural basis for recognition of CD20 by therapeutic antibody rituximab. *J Biol Chem.* 2007;282(20):15073-15080.
8. Du J, Wang H, Zhong C, et al. Crystal structure of chimeric antibody C2H7 Fab in complex with a CD20 peptide. *Mol Immunol.* 2008;45(10):2861-2868.
9. Polyak MJ, Deans JP. Alanine-170 and proline-172 are critical determinants for extracellular CD20 epitopes; heterogeneity in the fine specificity of CD20 monoclonal antibodies is defined by additional requirements imposed by both amino acid sequence and quaternary structure. *Blood.* 2002;99(9):3256-3262.
10. Teeling JL, Mackus WJM, Wiegman LJJM, et al. The biological activity of human CD20 monoclonal antibodies is linked to unique epitopes on CD20. *J Immunol.* 2006;177(1):362-371.
11. Slootstra JW, Puijk WC, Ligtvoet GJ, Langeveld JP, Meloen RH. Structural aspects of antibody-antigen interaction revealed through small random peptide libraries. *Mol Divers.* 1996;1(2):87-96.
12. Banyay M, Gilstring F, Hauzenberger E, et al. Three-dimensional imaging of in situ specimens with low-dose electron tomography to analyze protein conformation. *Assay Drug Dev Technol.* 2004;2(5):561-567.
13. Johnson NA, Leach S, Woolcock B, et al. CD20 mutations involving the rituximab epitope are rare in diffuse large B-cell lymphomas and are not a significant cause of R-CHOP failure. *Haematologica.* 2009;94(3):423-427.
14. Stanfield RL, Zemla A, Wilson IA, Rupp B. Antibody elbow angles are influenced by their light chain class. *J Mol Biol.* 2006;357(5):1566-1574.
15. Du J, Yang H, Guo Y, Ding J. Structure of the Fab fragment of therapeutic antibody Ofatumumab provides insights into the recognition mechanism with CD20. *Mol Immunol.* 2009;46(11-12):2419-2423.

2011 118: 358-367
doi:10.1182/blood-2010-09-305847 originally published online March 28, 2011

Epitope characterization and crystal structure of GA101 provide insights into the molecular basis for type I/II distinction of CD20 antibodies

Gerhard Niederfellner, Alfred Lammens, Olaf Mundigl, Guy J. Georges, Wolfgang Schaefer, Manfred Schwaiger, Andreas Franke, Kornelius Wiechmann, Stefan Jenewein, Jerry W. Slootstra, Peter Timmerman, Annika Brännström, Frida Lindstrom, Ekkehard Mössner, Pablo Umana, Karl-Peter Hopfner and Christian Klein

Blood (print ISSN 0006-4971, online ISSN 1528-0020), is published weekly by the American Society of Hematology, 2021 L St, NW, Suite 900, Washington DC 20036.